

## Optical Structure and Physics of the M87 Jet

Eric S. Perlman

*Joint Center for Astrophysics, University of Maryland, Baltimore  
County, 1000 Hilltop Circle, Baltimore, MD 21250 USA*

William B. Sparks, John Biretta, Duccio Macchetto

*Space Telescope Science Institute, 3700 San Martin Drive, Baltimore,  
MD 21218 USA*

J. Patrick Leahy

*University of Manchester, Jodrell Bank Observatory, Macclesfield,  
Cheshire, SK11 9DL, UK*

### Abstract.

We summarize HST observations of the M87 jet, concentrating on polarimetry and spectral index maps, and compare its optical and radio structures. The evidence now supports a stratified model for the structure of the jet, whereby high-energy, optical synchrotron emitting particles occupy physically different regions of the jet, closer to the jet axis, with different magnetic field configurations. It is in these regions where the shocks that produce the knots in the inner jet appear to originate. Knot regions have optical spectra which are much flatter than average for the jet, with the flattest-spectrum regions coinciding with flux maxima of knots. These same regions are preceded by regions where perpendicular magnetic fields are seen. Thus not only do we see all the necessary ingredients for *in situ* particle acceleration in the knots, but there is now fairly direct evidence for it as well. By tracking the changes in radio-optical and optical spectral index in the knot regions, we can comment on acceleration and cooling timescales in each knot.

### 1. Introduction

The giant elliptical galaxy M87 hosts the best-known extragalactic jet. Because of its proximity ( $D=16$  Mpc) and high surface brightness, in M87 we can study jet physics in far higher detail than is possible for any other source.

Since its launch, HST has studied M87 in great detail. A comparison of the jet's radio and optical structure (Sparks et al. 1996) finds remarkable large-scale similarity, but clear and significant differences appear on  $0.1''$  scales. The optical emission is more concentrated in knots and along the centerline, a trend which continues into the UV. All of the inner jet knots (i.e., interior to knot A), show apparent superluminal motion, with speeds ranging from  $2 - 6c$  (Biretta et al. 1999). The superluminal components vary significantly on 1 year timescales.

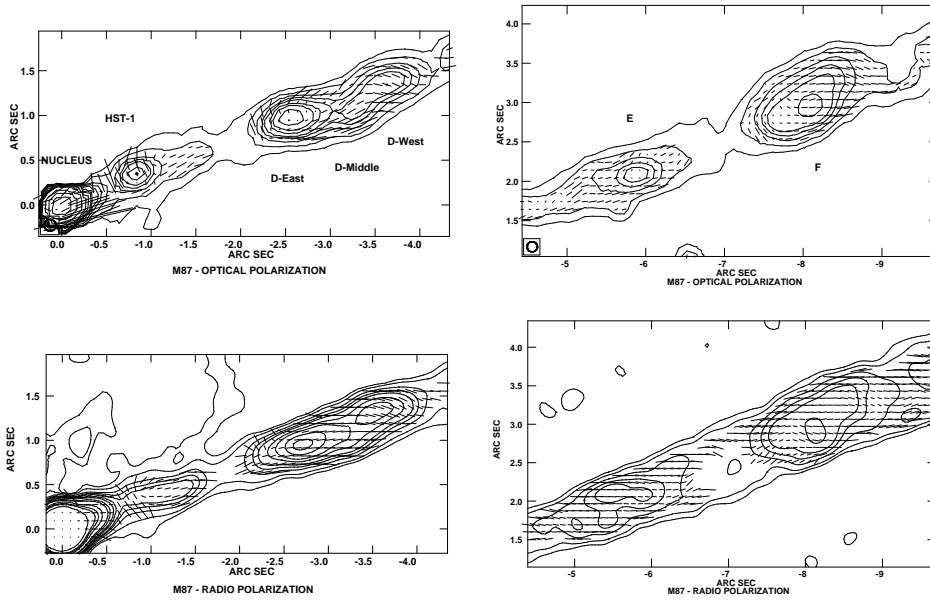


Figure 3

Figure 4

Figure 1. Polarization maps of the inner jet. North is at the top and East is at the left. The optical image is contoured at  $(1, 2, 4, 6, 8, 12, 16, 24, 32, 64, 128, 256) \times 50$  ADU/pix, while the radio image is contoured at  $(1, 2, 4, 6, 8, 12, 16, 24, 32, 64, 128, 256) \times 0.5$  mJy/beam. The vectors represent MFPA ( $1'' = 300\%$  polarization).

With this in mind, we discuss polarimetric and spectral index maps of the M87 jet. Polarimetry is by far the most sensitive probe of a jet's structure, because it tracks directly the structure of the magnetic field in the emission regions. The comparison of polarized structures in radio and optical bands is a particularly powerful tool, as it allows us to see whether the magnetic fields in those regions have similar or different properties. Spectral index images are equally powerful, as they allow us to view not only the spectrum of the emitted radiation, but also the underlying spectrum of the synchrotron emitting particles. A comparison of spectral index maps in two bands can diagnose the structure of the jet and the presence of particle acceleration.

Here we emphasize certain features in the polarization and spectral index images presented in Perlman et al. (1999, 2001), and discuss in particular the inner jet. For more detailed discussions, the reader is directed to those papers.

## 2. Maps and Results

In Figure 1, we show a comparison of radio and optical polarimetry in the inner regions of the M87 jet. Figure 2 compares the run of radio-optical and optical spectra with that of optical flux in these same regions.

Significant differences are evident in the optical and radio polarization structures of knots in the inner jet (Figure 1). The polarization varies far more in the optical than it does in the radio, with the strongest variations near the flux maxima. The average optical polarization just upstream of the flux peak in HST-1 is  $\langle P_{opt} \rangle = 0.45 \pm 0.08$ , while at the maximum,  $P_{opt}$  drops to just  $0.14 \pm 0.05$ . In D, E and F,  $P_{opt}$  values of 0.15 – 0.30 are observed just upstream of the flux peaks, compared with  $< 0.10$  at the flux peaks. By comparison,  $P_{rad}$  drops from  $\sim 0.25$  to 0.15 at the flux peak, a similarly small change is observed in F, and the drops in  $P_{rad}$  observed at the flux peaks of D and E are statistically insignificant. Obvious differences in the magnetic field orientation are also observed. Notably, at the upstream ends of knots HST-1, D and F, the optical magnetic field position angle (MFPA) becomes nearly perpendicular to the jet, whereas the radio MFPA remains primarily along the jet axis in D and F.

We also see clear differences in these regions between variations in  $\alpha_o$  and  $\alpha_{ro}$  (Figure 2). Much larger variations are observed in  $\alpha_o$  near flux maxima, than are seen in  $\alpha_{ro}$ . Bright regions of the knots have flatter  $\alpha_o$ , with particularly sharp variations in HST-1 and D. Those same regions have much smoother variations in  $\alpha_{ro}$ . Also,  $\alpha_o$  and  $\alpha_{ro}$  do not vary together in the knot regions. In two regions,  $\alpha_o$  appears to lead  $\alpha_{ro}$ : knot HST-1 (by  $0.15''$ ) and knot F (by  $0.2''$ ). But two other knots show just the opposite, with  $\alpha_o$  lagging  $\alpha_{ro}$ : knot D (by  $0.15''$ ) and knot E (by  $0.25''$ ) In addition, the flat- $\alpha_{ro}$  regions are larger than the corresponding flat- $\alpha_o$  regions, and significantly larger values of  $\alpha_{ro} - \alpha_o$  are observed immediately downstream of the flux maxima. But further downstream this steepening stops once the local mean in  $\alpha_{ro} - \alpha_o$  is reached.

### 3. Discussion

These data are hard to explain unless the jet is stratified, with high-energy electrons concentrated closer to the axis than lower-energy electrons (Perlman et al. 1999). Shocks appear to originate in the high-energy emitting regions, and thus we see rotations of the optical MFPA just upstream of the flux maximum. But at knot maxima, we see enhanced emission from both the jet center and edge, such that the polarization vectors cancel out in the optical but not in the radio. This model also predicts the much narrower flat- $\alpha_o$  regions that we see, and the relatively poor correlation between  $\alpha_o$  and  $\alpha_{ro}$ .

Given the perpendicular MFPA's we observe, the knots possess all the necessary ingredients for localized particle acceleration. Evidence for particle acceleration can be seen in the run of  $\alpha_o$  (Figure 2), which shows sharp flattenings beginning in the same regions where perpendicular MFPA's are observed, and the flattest spectra coinciding with flux maxima. It is hard to explain the runs of  $\alpha_o$  and  $\alpha_{ro}$  without invoking particle acceleration, because otherwise one would expect (1) no sharp variations in  $\alpha_o$  near flux maxima, (2)  $\alpha_o$  and  $\alpha_{ro}$  should vary together, and (3)  $\alpha_{ro} - \alpha_o > 0$  everywhere in the jet. Particle acceleration can easily account for the long-standing discrepancy (Meisenheimer et al. 1996 and refs. therein) between the particle ages ( $\sim 100 - 300$  years) and length of the jet (2 kpc), without requiring that the jet be as strongly out of equipartition as suggested by Heinz & Begelman (1997). Indeed, particle acceleration is expected in these knots if they are analogous to flaring regions in blazar jets.

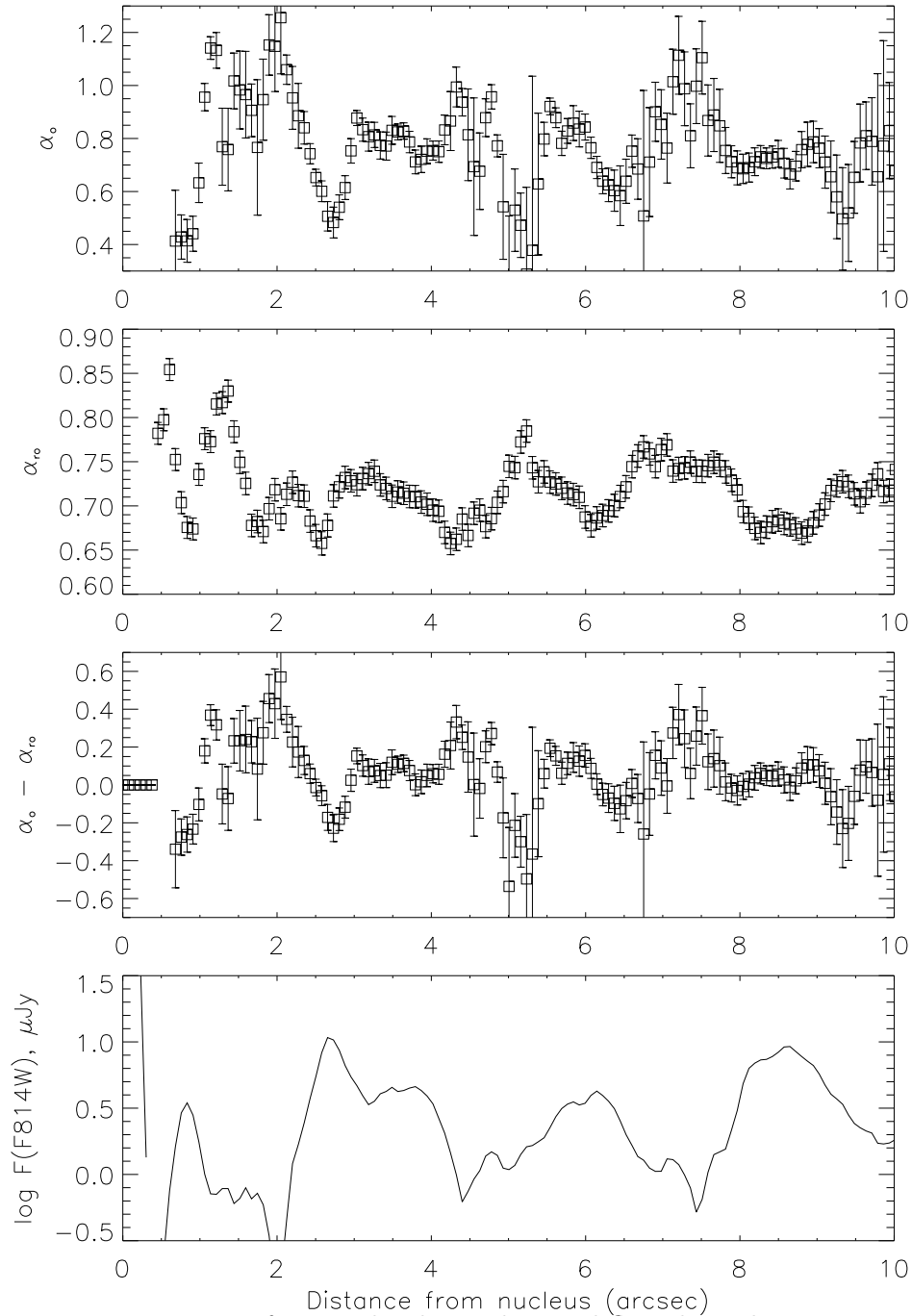


Figure 2. Runs of spectral index and optical flux along the jet axis. Only the inner jet region is shown. As can be seen, much stronger spectral variations are seen in  $\alpha_o$  than  $\alpha_{ro}$ , and the two spectral indices do not vary in a correlated fashion near flux maxima.

If particle acceleration is present, the runs of  $\alpha_o$  and  $\alpha_{ro}$  represent a time history of particle acceleration and synchrotron aging. In two knots (D-East and E), we observe  $\alpha_{ro}$  leading  $\alpha_o$ , while in two others (HST-1 and F), the opposite is observed. Both are consistent with models for flares produced by shock-induced particle acceleration. As Kirk et al. (1998) showed, the evolution of spectral index in a given band during a flare depends on the relationship of the acceleration and cooling timescales  $t_{acc}$  and  $t_{cool}$  for electrons which emit in that band. Where  $t_{acc}$  is much shorter than  $t_{cool}$ , higher-energy emissions should lead lower-energy emissions (Georganopoulos & Marscher 1998, Takahashi et al. 1999). But if  $t_{acc}$  and  $t_{cool}$  are close to equal near the peak in  $\nu F_\nu$ , things are more complex. At low energies, where  $t_{acc}$  is much faster than  $t_{cool}$  (n.b.,  $t_{cool} \propto E_\gamma^{-1/2}$ ), the spectrum should flatten in advance of the flux maximum, peaking slightly before flux maximum, followed by a steepening to values somewhat below the jet's nominal value after maximum flux, and then a return to the nominal value after the disturbance has passed. But at high energies, where  $t_{cool} \sim t_{acc}$ , spectral *steepening* is predicted in advance of the flux maximum, followed by a hardening as the number of newly accelerated electrons build up. Under this model (assuming no injection of fresh particles), flares represent the reacceleration of old particles within the jet, so they will propagate from low to high energies, *i.e.* observed spectral changes at higher energies will lag those at lower energies. We appear to be observing *both* situations in different knot regions in the M87 jet.

## References

- Biretta, J. A., Sparks, W. B., & Macchetto, F. D., 1999, ApJ, 520, 621  
 Georganopolous, M., & Marscher, A. P., 1998, ApJ 506, L11.  
 Heinz, S., & Begelman, M. C., 1997, ApJ 490, 633.  
 Kirk, J. G., Rieger, F. M., & Mastichiadis, A., 1998, A & A 333, 452.  
 Meisenheimer, K., Roeser, H.-J., & Shlötelburg, M., 1996, A&A 307, 61.  
 Perlman, E. S., Biretta, J. A., Zhou, F., Sparks, W. B., & Macchetto, F. D., 1999, AJ 117, 2185  
 Perlman, E. S., Biretta, J. A., Sparks, W. B., Macchetto, F. D., & Leahy, J. P., 2001, ApJ, in press (astro-ph/0012044).  
 Sparks, W. B., Biretta, J. A., & Macchetto, F., 1996, ApJ 473, 254.  
 Takahashi, T., Madejski, G., & Kubo, H., 1999, Astroparticle Physics 11, 177.